

## Supporting Information

### **Facile Synthesis of Biogenic Silica Nanomaterial Loaded Transparent Tragacanth Gum Hydrogel with Improved Physico-Chemical and Inherent Anti-Bacterial Activity**

Mohini Verma<sup>1,2</sup>, Aqib Iqbal Dar<sup>1,2</sup> and Amitabha Acharya<sup>1,2\*</sup>

*<sup>1</sup>Biotechnology Division, CSIR-Institute of Himalayan Bioresource Technology, Palampur (H.P.) 176061, India*

*<sup>2</sup>Academy of Scientific & Innovative Research (AcSIR), Ghaziabad-201002, India*

\*Author to whom the correspondence should be addressed, E-mail:

[amitabhachem@gmail.com](mailto:amitabhachem@gmail.com); [amitabha@ihbt.res.in](mailto:amitabha@ihbt.res.in); Tel (off): +91-1894-233339; Extn. 397;

Fax: +91-1894-230433

## Table of content

SI No.	Content	Page No.
<b>S1</b>	Experimental methods S1. (a) Characterization method (Table S1) S1. (b) Quantitative and qualitative determination of quaternary ammonium salt (QAS) concentration in CTAB@BSNP and CTAB@BSNP-TG hydrogel S1. (c) Studies on water retention capacity of the prepared hydrogels (Swelling index). S1. (d) Injectability studies of the developed hydrogels. S1. (e) Antibacterial activity of the developed BSNP, CTAB@BSNP and APTES@BSNP S1. (f) Bacterial surface charge measurement using zeta potential. S1. (g) Determination of minimum inhibitory concentration. S1. (h) Rheological evaluation S1. (i) Secondary penetration assay S1 (j) Membrane depolarization assay (DiSC <sub>3</sub> 5) S1. (k) Antifouling activity of hydrogel S1. (l) Effect of hydrogel on collagen secretion S1. (m) Self-healing of hydrogel	S3-S7
<b>Table S2</b>	Different conditions used for silica isolation	S8
<b>Table S3</b>	Different methods for modifying BSNP	S9
<b>Table S4</b>	Hydrogel formation varying concentration of NPs	S10
<b>Table S5</b>	Isolation of Silica NPs from different plant species	S11
<b>Figure S1</b>	Chemical structures, EDAX and SAED pattern of functionalized NPs	S12
<b>Figure S2</b>	Zeta potential studies	S13
<b>Table S6</b>	Crystallinity index of NPs	S13
<b>Figure S3</b>	XPS studies	S14-S15
<b>Table S7</b>	Different application areas for TG gel	S16
<b>Table S8</b>	Hydrogel film formation varying temperature conditions	S17
<b>Table S9</b>	Hydrogel film formation varying components	S18
<b>Figure S4</b>	SEM and EDAX studies of hydrogel, Zeta potential, Bromophenol blue assay, Strain-dependent oscillatory rheology	S19-S20
<b>Figure S5</b>	Antibacterial activity of NPs	S21
<b>Figure S6</b>	NPs-bacteria interaction study via zeta potential	S22
<b>Figure S7</b>	Secondary penetration	S23
<b>Figure S8</b>	Cell migration assay	S24
<b>References</b>		S25-S28

## S1 Experimental section

### S1. (a) Characterization methods

Table S1.

Characterization techniques	
1.	Transmission electron microscope (TEM)
2.	Fourier-transform infrared spectroscopy
3.	X-ray photoelectron spectroscopy (XPS)
4.	Powder X-ray diffraction (P-XRD)
5.	Zeta potential
6.	Scanning Electron Microscope (SEM)

The morphological analysis of BSNP and their chemical counterparts *viz.*, CTAB@BSNP and APTES@BSNP was done using transmission electron microscope (TEM, Tecnai Twin 200 kV, FEI, Netherlands). For TEM a drop of the sample (1mg/mL) was placed on a carbon-coated copper grid. The sample was dried at room temperature and imaged at desired magnifications. FTIR analysis of nanoparticles (NPs) and hydrogel was done using Shimadzu IRAffinity-1S at the scanning wavelength range of 4,000-400cm<sup>-1</sup> and the corresponding peaks were assigned accordingly. The X-ray photoelectron spectroscopy (XPS) was done using Thermo Fisher Scientific Nexsa base whereas the powder X-ray diffraction (P-XRD) was done using Rigaku-Smart Lab 9kW rotating anode X-ray diffractometer. Zeta potential studies have been done using Zetasizer Nano ZS (Malvern Instruments). For this, in a zeta cuvette, 1 ml sample solution (1mg/mL) was taken and at least three measurements were done. In case of hydrogels *viz.*, TG, BSNP-TG, APTES@BSNP-TG and CTAB@BSNP-TG were taken in zeta cuvette and three measurements were done. Further, the morphological analysis of hydrogel was done using Scanning Electron Microscope (SEM, Hitachi S-3400N).

**S1.(b) Quantitative and qualitative determination of quaternary ammonium salt (QAS) in CTAB@BSNP and CTAB@BSNP-TG hydrogel respectively.** The QAS (CTAB) present on the surface of CTAB@BSNP and CTAB@BSNP-TG was determined using

bromophenol blue (BPB) dye. By varying different concentrations of CTAB, a standard curve was plotted. The quantification of CTAB present in the CTAB@BSNPs was done from the standard plot. Presence of CTAB in CTAB@BSNP-TG was qualitatively monitored by the colour change (purple to blue) which is due to the interaction of BPB with the QAS containing moiety. For this, 100 $\mu$ L of bromophenol blue dye (0.1mg/mL) was spread and change in colour was observed for all the hydrogels.<sup>1</sup>

**S1.(c) *Studies on water retention capacity of the prepared hydrogels (swelling index).*** The swelling index of the hydrogel was determined by placing a block of dry hydrogels (2 $\times$ 2 cm, weight measured) viz., TG, BSNP-TG, CTAB@BSNP-TG and APTES@BSNP-TG into measured amount of DDW and 0.85% NaCl solution, respectively and the total solution was placed at 37 $^{\circ}$ C for 12 h. After every 2h of incubation, hydrogels were wiped thoroughly and the corresponding weight was checked. This process was repeated several times until a constant weight was obtained for the hydrogel. This experiment was carried out with three different block hydrogels of similar dimensions (for all the gels) to obtain reproducibility. The swelling index was calculated according to equation (1).

$$\text{Swelling index} = \frac{(\text{Swelled hydrogel} - \text{dry hydrogel})}{\text{dry hydrogel}} \times 100 \quad (1)$$

**S1.(d) *Injectability studies of the developed hydrogels.*** For evaluating the injectability of the developed hydrogels viz., TG, BSNP-TG, APTES@BSNP-TG and CTAB@BSNP-TG the respective hydrogel casting solutions were taken in a 5 mL syringe, incubated at 37 $^{\circ}$  C for 8h and the corresponding gel was injected out of the injection nozzle to check its consistency. Similar studies were also performed using methylene blue as a staining dye to obtain coloured gels.

**S1.(e) Antibacterial activity of the developed BSNP, CTAB@BSNP and APTES@BSNP.**

The disc diffusion method was employed to check the antibacterial efficacy of the NPs against two different bacterial strains *viz.*, Gram-positive *Staphylococcus aureus* (MTCC 3160) and Gram-negative *Pseudomonas aeruginosa* (MTCC 741).<sup>2,3</sup> The single colony of bacteria *S. aureus* (MH media) and *P. aeruginosa* (LB media) were inoculated in their respective media (10mL) and were incubated at 180 rpm at 37°C overnight to allow cell growth. The concentration (OD<sub>600</sub>) of the bacteria was adjusted to 0.08-0.1 and this was used for further studies. The MH and LB plates were inoculated with a 20 µl (10<sup>5</sup> CFU/ ml) culture of *S. aureus* and *P. aeruginosa*, respectively. The cultures were spread on the plate with the help of L-shaped sterile spreader. The plates were kept overnight at 37°C and the corresponding zone of inhibition was observed.

**S1.(f) Bacterial surface charge measurement using zeta potential.** Both bacteria (*P. aeruginosa* and *S. aureus*) were suspended in PBS buffer (OD<sub>600</sub>, 0.1) were incubated with BSNP, APTES@BSNP, CTAB@BSNP for 4h at 180rpm. Change in surface charge before and after the treatment incubation was measured by DLS/zeta instrument.<sup>4</sup>

**S1.(g) Determination of minimum inhibitory concentration (MIC).** This was performed according to our previous report.<sup>2</sup> Briefly, different concentrations *viz.*, 50, 100, 150, 200 and 300 µg/mL of nanomaterials *viz.*, BSNP, CTAB@BSNP and APTES@BSNP were added to 100 µL of overnight grown both the bacterial culture of fixed concentration in a 96 well plate. The corresponding volume makeup was done using the growth media. This mixture was then placed in an incubator at 37°C at 180 rpm. The corresponding reading was (OD<sub>600</sub>) were taken after every 2 h interval and MIC was calculated.

**S1.(h) Rheological evaluation.** The viscosity of hydrogel was determined to characterize gelation temperature. The viscometer (IKA Rotavisc lo-vi, Germany) was preheated before characterization. The solution was prepared and 100 mL of each sample was transferred to

the viscometer. Viscosity was measured at various temperature intervals starting from high temperature. The router speed was set at 10 rpm and the measurement was tested 3 times.

The Oscillatory shear rheology measurements were evaluated using Anton Paar Modular Compact Rheometer MCR102 (measuring system; PP50, frequency; 1.59 Hz, probe gap; 1mm and software; Rheocompass). All the freshly prepared hydrogel were directly placed on the metal stage of the rheometer and silicon oil was used to prevent water evaporation. Further, the probe was lowered and displacements were taken every 60s. The linear viscoelastic range (DLVR) of the prepared hydrogels was determined using frequency sweep test. While the sample was set in its equilibrium state, the stress progression was evaluated by subjecting to a constant shear rate. All measurements were carried out at 25°C. Further, strain sweep of loss to the storage or damping ( $\tan \delta$ ) was evaluated from 0-1000% of the strain.<sup>5,6</sup>

**S1.(i) *Secondary penetration assay.*** Microbial penetration in presence of hydrogel was tested to check the hydrogel film efficiency to inhibit the secondary wound infection. For this, autoclaved growth media in pre-autoclaved test tubes was taken and the opening of the tubes was sealed with the help of each hydrogel films. Turbidity of the growth media present in a test tube was monitored after incubating these at 37°C for 15 days. All tests were repeated in triplicates.<sup>7</sup>

**S1.(j) *Membrane Depolarization Assay.*** 3,3'-Dipropylthiadicarbocya nine iodide (DiSC<sub>3</sub>5) is a cationic membrane potential sensitive dye that is known to accumulate on hyperpolarized membranes and demonstrate diminished fluorescence upon integration to the bacterial membrane. DiSC<sub>3</sub>5 was utilised to investigate the depolarization of the bacterial membrane caused by our hydrogels. *S. aureus* and *P. aeruginosa* was kept to grow upto mid log phase (O.D- 0.5). Bacteria were centrifuged at 5000 rpm for 3min which were then washed and resuspended in HEPES buffer (5 mM HEPES, 20 mM glucose, pH 7.4). DiSC<sub>3</sub>5 (1 $\mu$ M) was added to the cell solution and incubated for 1 hour at 37°C before adding 100 mM KCl and

incubating for 15 minutes. After that, cells were treated with 30mg/ml of each hydrogel. Readings were taken with fluorescence emission at 670 nm and excitation at 622 nm.<sup>20</sup>

**S1.(k) Antifouling activity of hydrogel.** For evaluating the antifouling property of hydrogel, it was cut into size of 2cm × 2cm pieces (weight ~30mg) and incubated in Nutrient Broth and Muller Hinton broth containing  $1 \times 10^8$  CFU/mL of *P. aeruginosa* and *S. aureus*, respectively. Samples were incubated at 37°C for 12h, after that washing was done with PBS thrice. Later on, samples were stained using Syto9 and propidium iodide (live/dead staining kit) and observed under fluorescence microscopy.<sup>8</sup>

**S1.(l) Effect of hydrogels on collagen secretion.** For the qualitative and quantitative estimation of the collagen secretion from NIH-3T3 fibroblast cells, we have employed both the spectroscopy and microscopy methods respectively. For both the methods, the cells were first seeded in a 12 well plate (20,000 cells/ well) and then allowed to grow for 24h. Treatment with hydrogels was given for 6h followed by washing. Then picosirius red was used for staining followed by washing with 10mM HCl and 0.1M NaOH. Finally, absorbance was taken at 540nm. For microscopic imaging, cells were grown over cover slip coated with poly L-lysine for 24h. Treatment with hydrogels was given for 6h followed by washing and staining. Staining was done using Hematoxylin (Harris) and picosirius red.<sup>9,10</sup> and finally the imaging was done using bright field microscope.

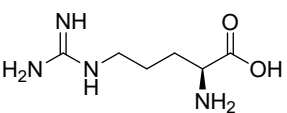
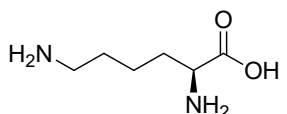
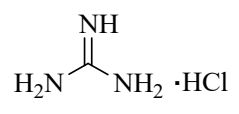
**S1.(m) Self-healing of hydrogel.** The freshly prepared hydrogel (CTAB@BSNP-TG) was cut into three parts and then these were kept in proximal contact with each other in a controlled environment at room temperature and then transferred to a beaker containing water and kept for 20 hours. The hydrogels were then held against gravity and placed to better demonstrate the gel's self-healing activity.<sup>21</sup>

**Table S2.** Different conditions used for silica isolation from *Lantana camara*

Calcination time/Temp. (Muffle furnace)	Acid reflux before calcination	HCl:H <sub>2</sub> SO <sub>4</sub> treatment before calcination	HCl:H <sub>2</sub> SO <sub>4</sub> treatment after calcination	NaOH (1M) treatment during calcination	NaOH treatment (conc./ time)	BSNP formation
7h/ 900°C	X	X	✓	X	(1M/ 24h)	✓*
4h/ 600°C	X	✓	X	X	(3.5 M/ 2h)	X
4h/ 600°C	✓	X	X	X	(3.5 M/ 2h)	X
4h/ 600°C	X	X	X	✓	X	X
7h/ 900°C	X	X	✓	X	(1M/ 24h)	✓#

X -- Absence    ✓ -- Presence    ✓\* -- % yield ~75±5 % yield    ✓# -- % yield ~72± 7%

**Table S3.** Different chemical methods used for conjugation of Bowknot silica nanoparticles (BSNP)

S. No.	Chemical moiety	Process (% yield)	Surface modification	Si-O-Si peak in FTIR
1.	CTAB	n-butyl alcohol and distilled water (1:1) was taken (pH-4 via formic acid). CTAB was added followed by BSNP's. solution kept at 60°C in stirring condition at rpm 300 for 12 hrs. Neutralize the solution by dialyzes against distilled water. Filter the solution and kept for drying (~82%).	✓	✓
2.	APTES	BSNP's were added in 10ml of pure ethanol containing 300 µl Ammonium hydroxide solution (30%). APTES was added slowly to the solution having temperature 80°C, rpm 250 for 48 hrs. washing was done by centrifuge at 15000 rpm for 10 min (~78%).		✓
3.	L-Arginine (R) 	L-Arginine was added in HEPES buffer (pH- 9) then BSNP were added and stir for 12h at RT. Later the solution was centrifuged at 10,000rpm for 15 min.	X	X
4.	L-Lysine (K) 	L-Lysine was added in HEPES buffer (pH- 9) then BSNP were added and stir for 12h at RT. Later the solution was centrifuged at 10,000rpm for 15 min.	X	X
5.	Guanidine hydrochloride (G-HCl) 	BSNP were added in 100mL cyclohexane, 2mL n-Hexanol, 2mL Triton-X-100, water added and stirred for 20min, 29% NH <sub>4</sub> OH added and stirred for 1h. guanidine hydrochloride was added and stirred for 24h. filtrate was washed with acetone and ethanol.	X	X

**Table S4. Gelation time required for the formation of different hydrogels at three different NPs concentrations**

Name	Room temperature (25°C)	Gelation time (h)	37°C	Gelation time (h)
TG	X	—		~24
1% BSNP-TG	✓	~18		~12
3% BSNP-TG		~14		~9
5% BSNP-TG		~14		~9
1% APTES@BSNP-TG	✓	~12		~8
3% APTES@BSNP-TG		~10		~6
5% APTES@BSNP-TG		~10	✓	~6
1% CTAB@BSNP-TG	✓	~10	✓	~7
3% CTAB@BSNP-TG	✓	~8	✓	~4
5% CTAB@BSNP-TG	✓	~8	✓	~4

**Table S5.** Comparison of silica NPs isolation processes from different plant species

S.No	Plant species	Monocot/ Dicot	Method used	Amorphous/ Crystalline	% Yield	Advantages	Disadvantages	References
1	<i>Saccharum officinarum</i> (Sugarcane)	Monocot	Surfactant mediated synthesis from sodium silicate	Amorphous	~88.7	Reusability of NPs	More number of steps and chemicals required	11
2	<i>Oryza sativa</i> (Rice)	Monocot	Microwave-assisted synthesis	Amorphous	~95	Short time reaction conditions	Amorphous form of silica NPs	12
3	<i>Zea mays</i> (Corn)	Monocot	Biogenic synthesis via biocatalyst <i>Fusarium culmorum</i>	Amorphous	~47±1.4	Spherical shaped NPs formed from amorphous form	Conversion efficiency to NPs is less	13
4	<i>Triticum</i> (wheat)	Monocot	Acidic treatment, heating, purification	Amorphous	~48.1±2	Lesser no. of synthesis steps	Unstructured shape, aggregated nanoparticles	14
5	<i>Bambusoideae</i> (Bamboo)	Monocot	Sintering, Acid-base treatment	Amorphous	~52	Simple synthesis protocol	Agglomerated clustered nanoparticles	15
6	<i>Lantana camara</i> (Weed)	Dicot	Calcination, Acid-base leaching	Crystalline (~60.6%)	~75±5	Crystalline BSNP with simple and cheap synthesis process	—————	Present work

**Figure S1**

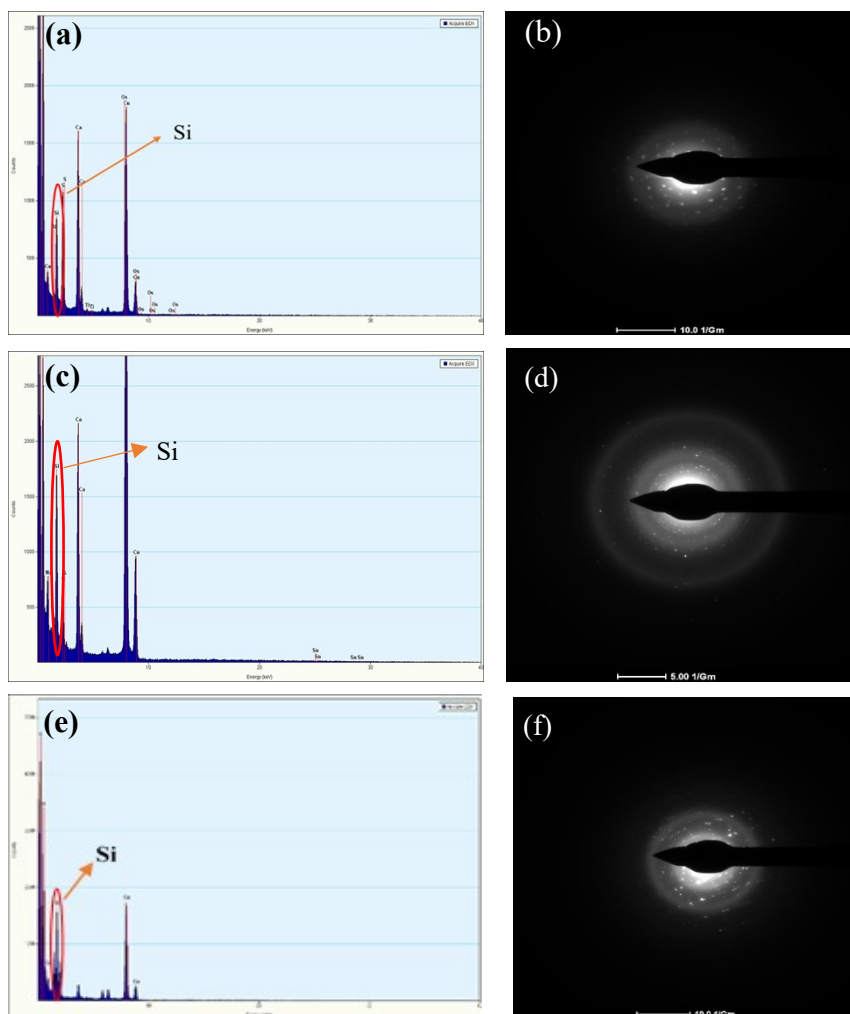


**Figure S1** (a), (c) and (e) EDAX of BSNP, APTES@BSNP and CTAB@BSNP, respectively. (b), (d) and (f) SAED pattern of BSNP, APTES@BSNP and CTAB@BSNP, respectively

**Figure S2.**

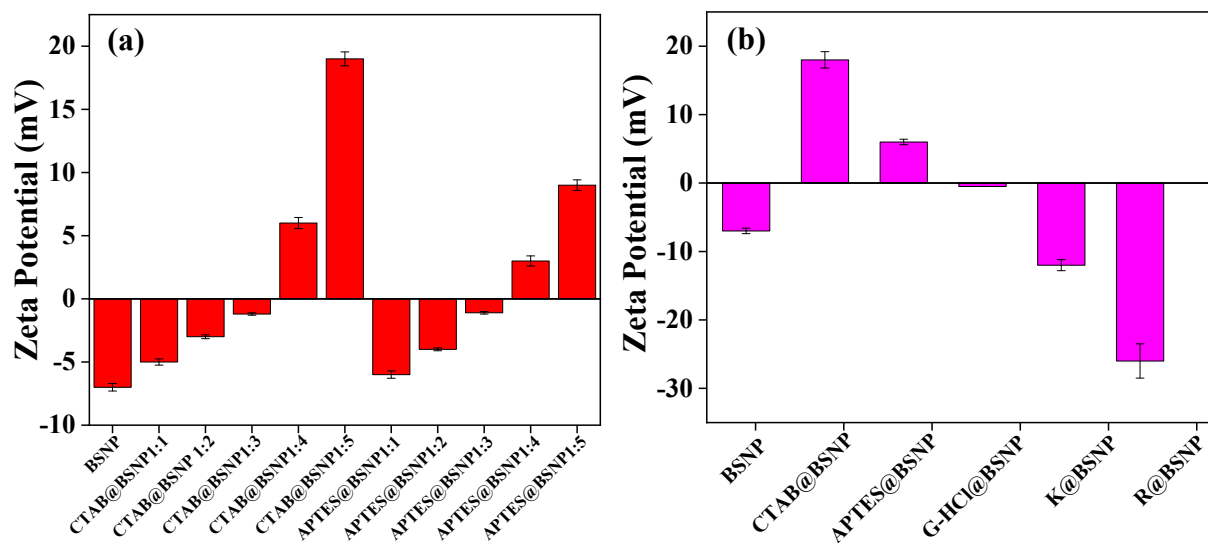
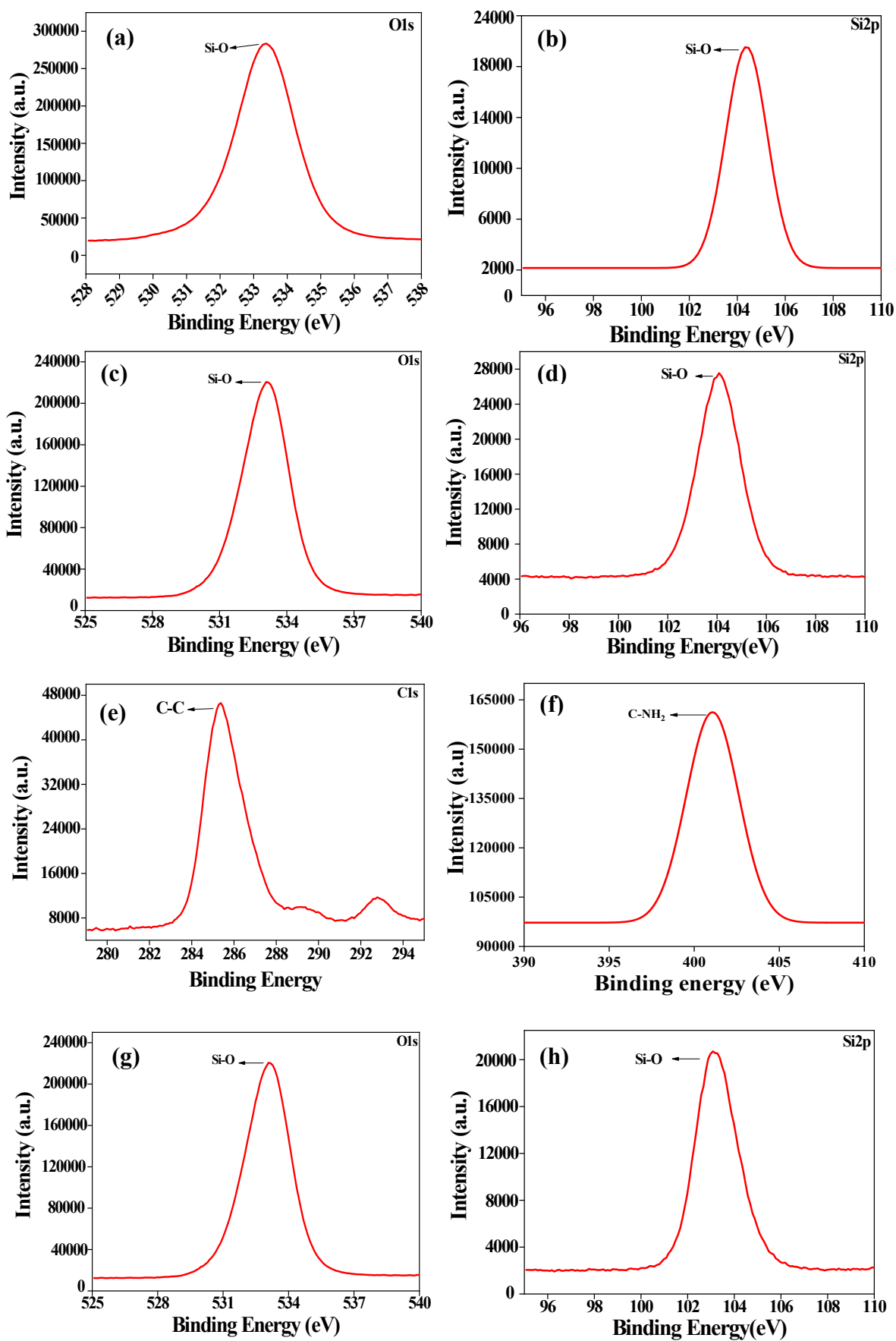


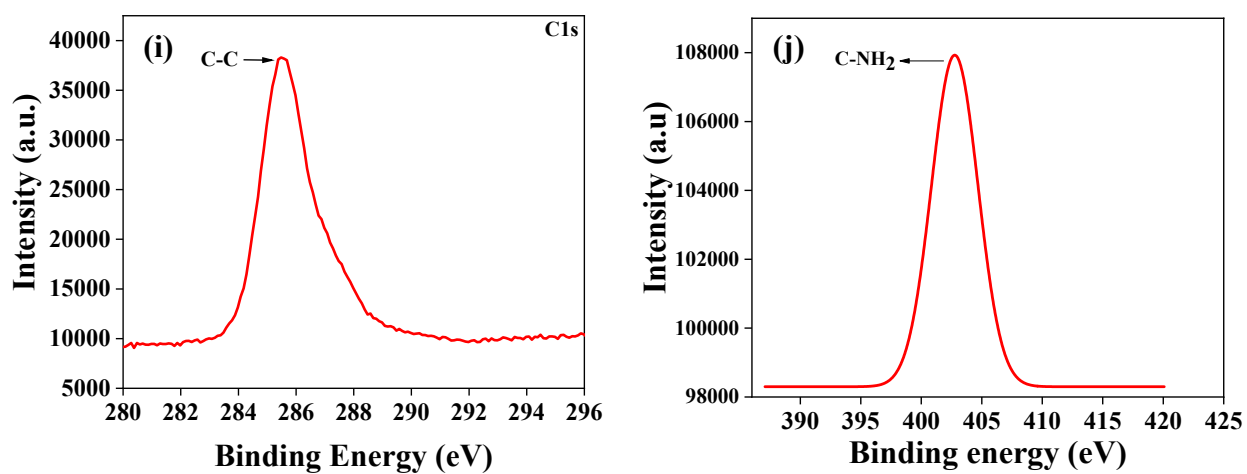
**Figure S2.** (a) Zeta potential studies of different ratios of APTES and CTAB with respect to BSNP, (b) Zeta potential studies of the chemical modified BSNP.

**Table S6.** Crystallinity index of the BSNP calculated from powder XRD studies

NPs	Crystallinity index (%)
BSNP	$\sim 60.5 \pm 2\%$
APTES@BSNP	$\sim 64 \pm 3$
CTAB@BSNP	$\sim 58 \pm 1.5$

Figure S3



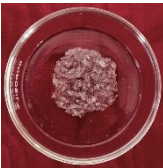
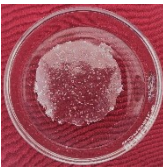
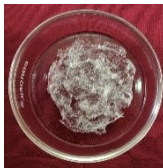


**Figure S3.** XPS spectra of (a, b) BSNP, (c-f) APTES@BSNP and (g-j) CTAB@BSNP.

**Table S7.** Literature reports for the use of different hydrogels.

<b>Hydrogel material</b>	<b>Crosslinking agent</b>	<b>NPs</b>	<b>Water retention/mechanical strength</b>	<b>Application</b>	<b>Reference</b>
TG and konjac glucomannan	Physical crosslinking	X	G' & G'' Vs Strain, flow point (~100%)	Thermosensitive hydrogel	16
TG and alginate gum	Radiation induced copolymerization	X	Swelling (~4%)	Wound healing	7
TG	Hydrogen bonding & electrostatic interaction	Modified CaCO <sub>3</sub> NPs	~468 mgg <sup>-1</sup>	Methylene blue adsorption	17
keratin/bacterial cellulose fibers, TG hydrogel	Non-ionic copolymerization	X	Tensile strength: 35%	Wound healing	18
TG, PVA, sodium alginate	Radiation	X	Swelling (~13.8%)	Wound healing	19

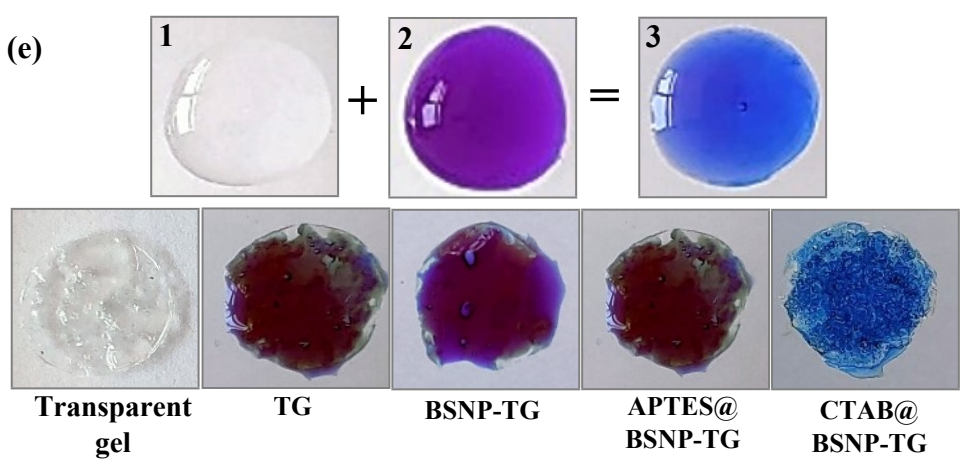
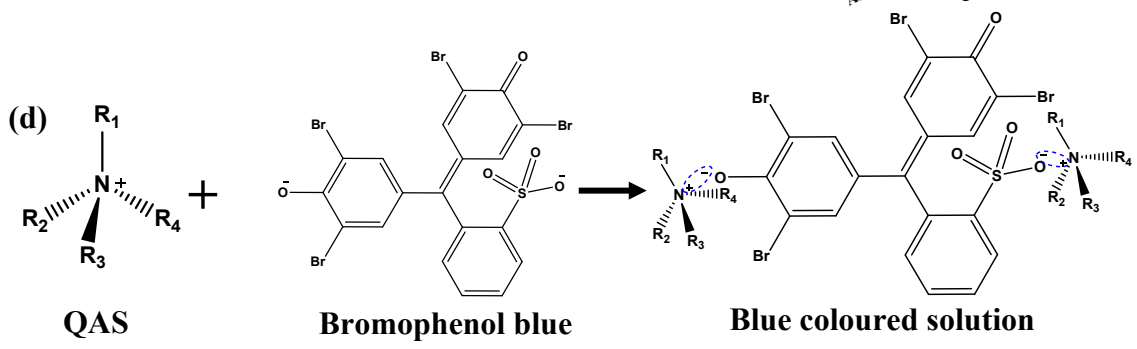
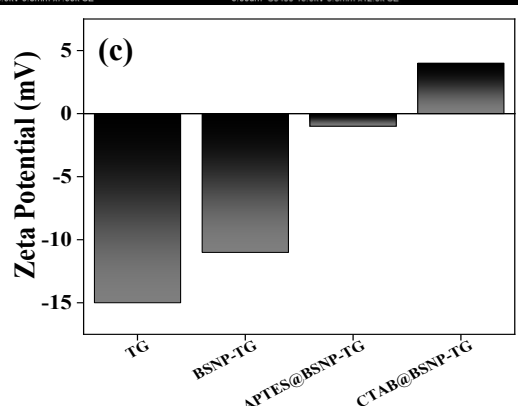
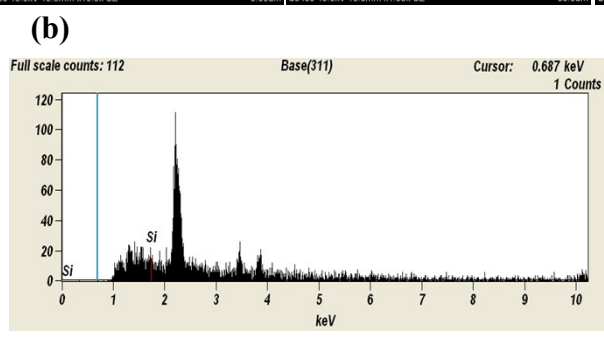
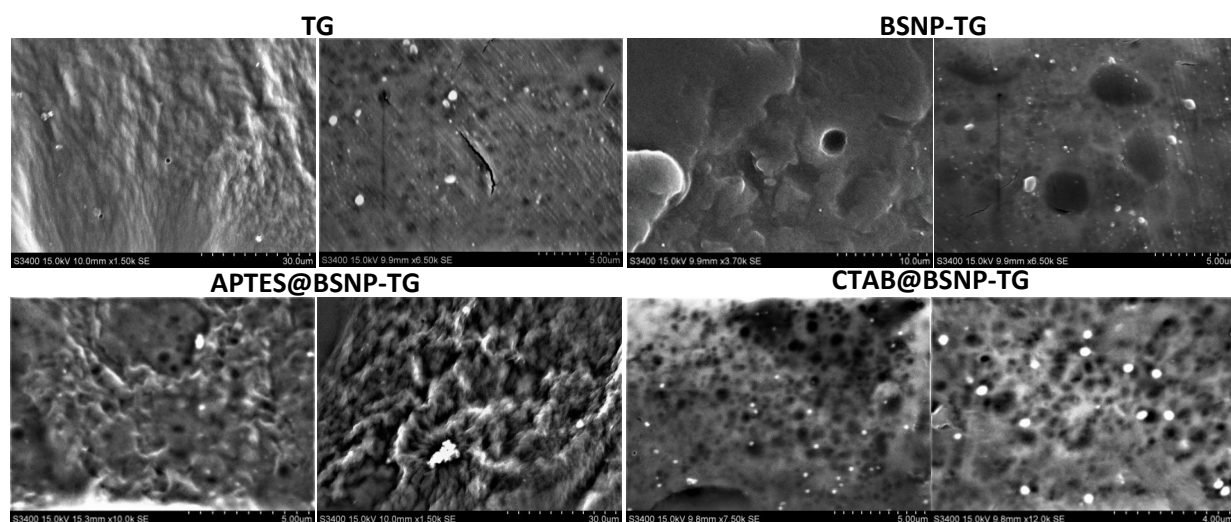
**Table S8.** Hydrogel film formation at varying temperature conditions

Name	4°C	37°C	70°C (Film formed is stiff in nature)
TG	X		
BSNP-TG	X		
APTES@BSNP-TG	X		
CTAB@BSNP-TG	X		

**Table S9.** Hydrogel film formation at varying gel components

TG	PVA	Glycerol	NPs	Gel strength
			<b>X</b>	 <b>Weak</b>
		<b>X</b>		 <b>Medium</b>
				 <b>Strong</b>
	<b>X</b>			<b>X</b>
	<b>X</b>		<b>X</b>	<b>X</b>
	<b>X</b>	<b>X</b>	<b>X</b>	<b>X</b>
	<b>X</b>	<b>X</b>		 <b>Weak</b>

Figure S4



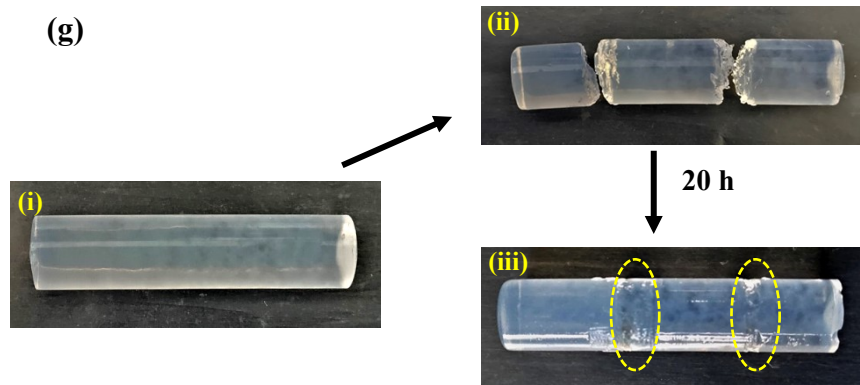
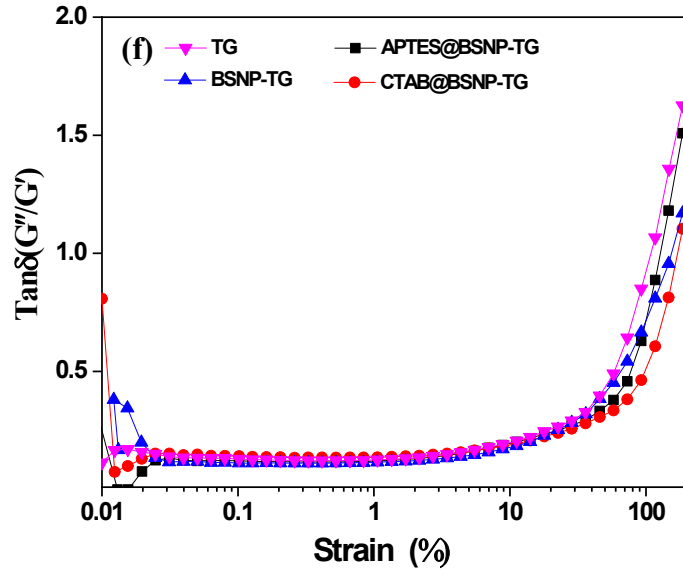


**Figure S4.** (a) SEM micrographs of TG, BSNP-TG, APTES@BSNP-TG, CTAB@BSNP-TG. (b) EDAX CTAB@BSNP-TG and (c) zeta potential studies of TG and modified hydrogels. (d) Reaction scheme for the interaction of quaternary ammonium salt (QAS) with bromophenol blue. (e) Colour change studies in the presence of bromophenol blue, where (1) CTAB solution, (2) Bromophenol blue, (3) mixture of (1) and (2) gives blue colour on interaction. (f)  $\tan \delta$  values of hydrogels. (g) Self-healing of CTAB@BSNP-TG hydrogel: (i) hydrogel, (ii) spliced hydrogel (iii) Self healed hydrogel.

Figure S5.

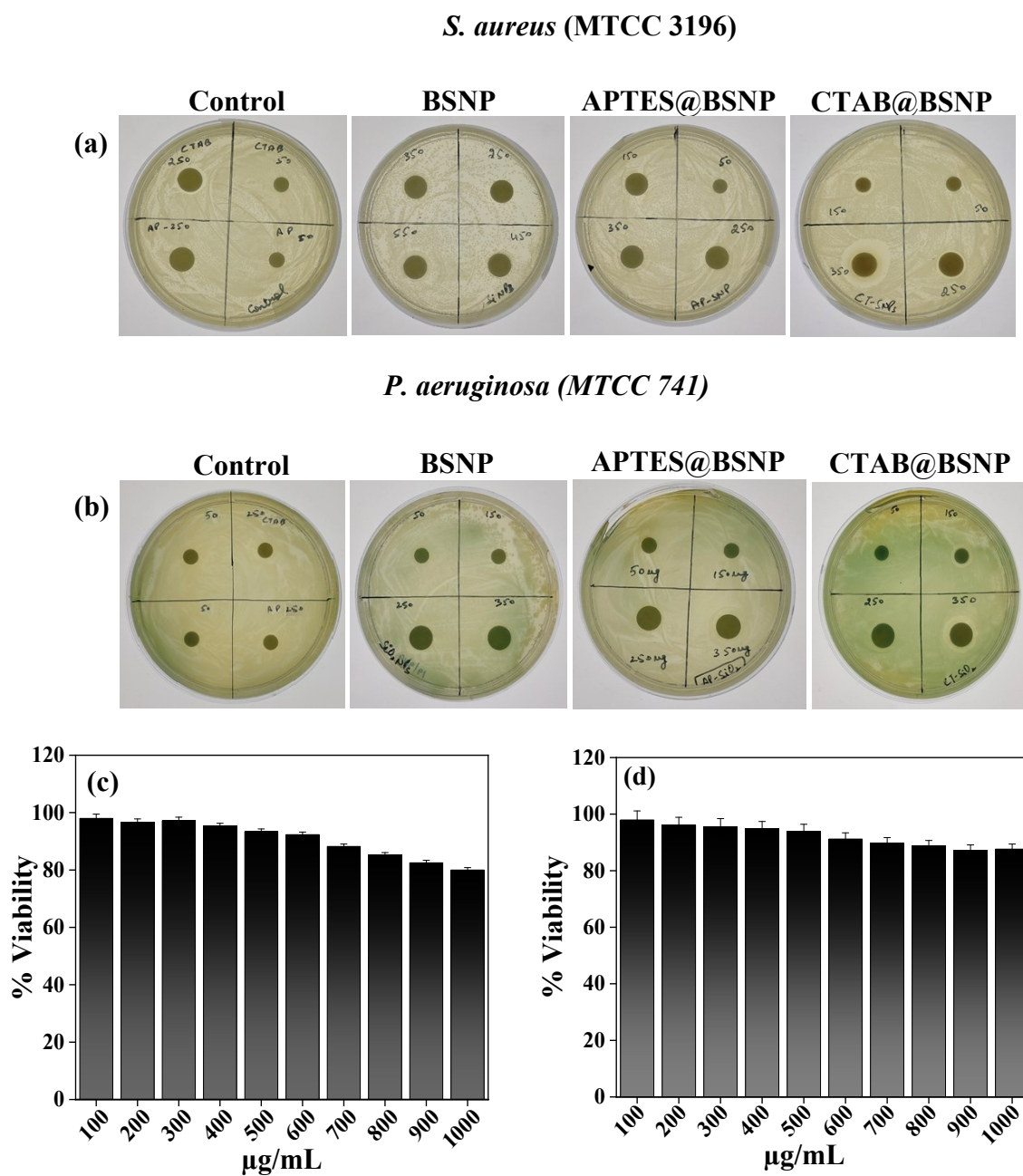
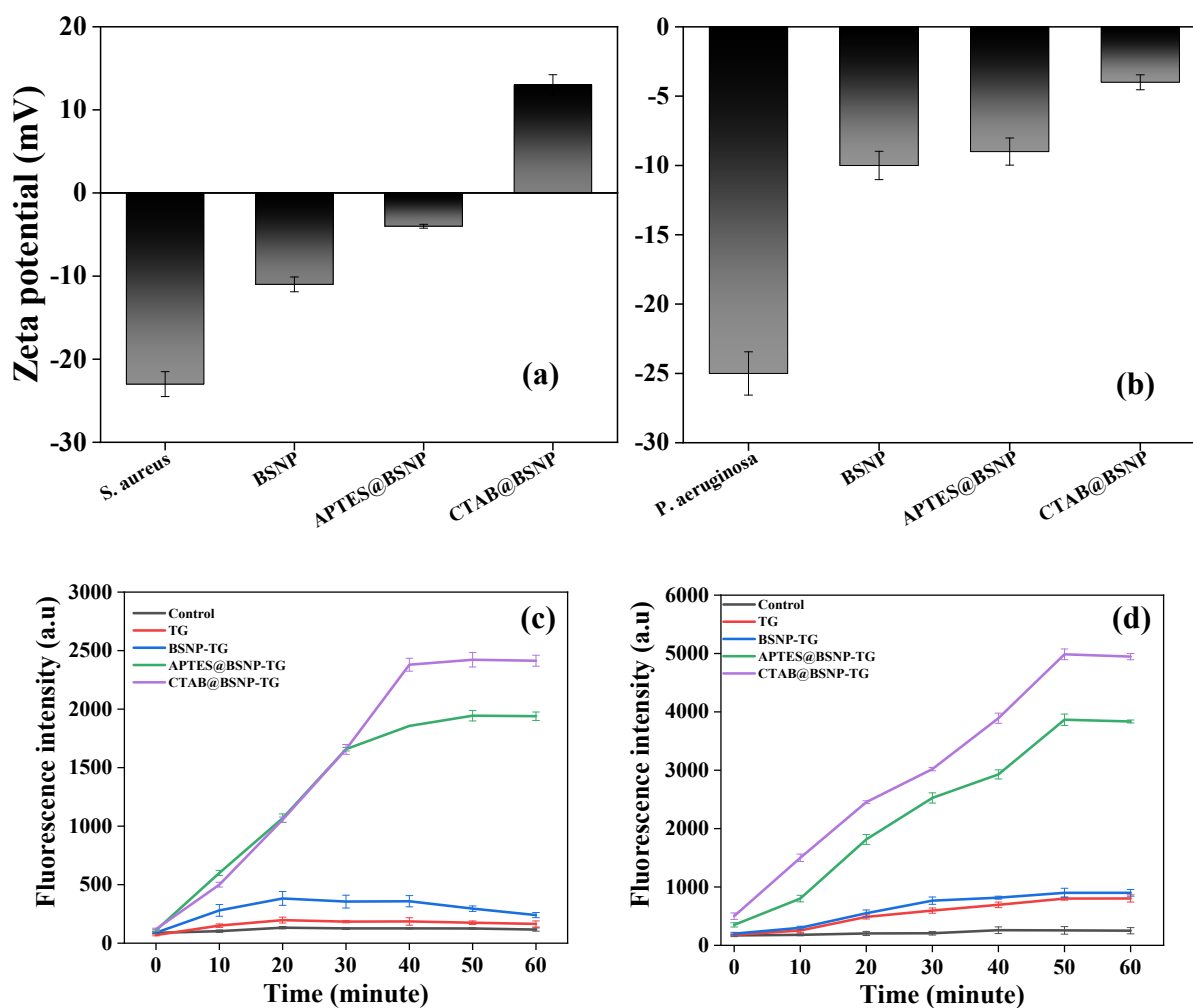


Figure S5. Antibacterial activity of NPs against (a) *S. aureus* and (b) *P. aeruginosa*. (c)

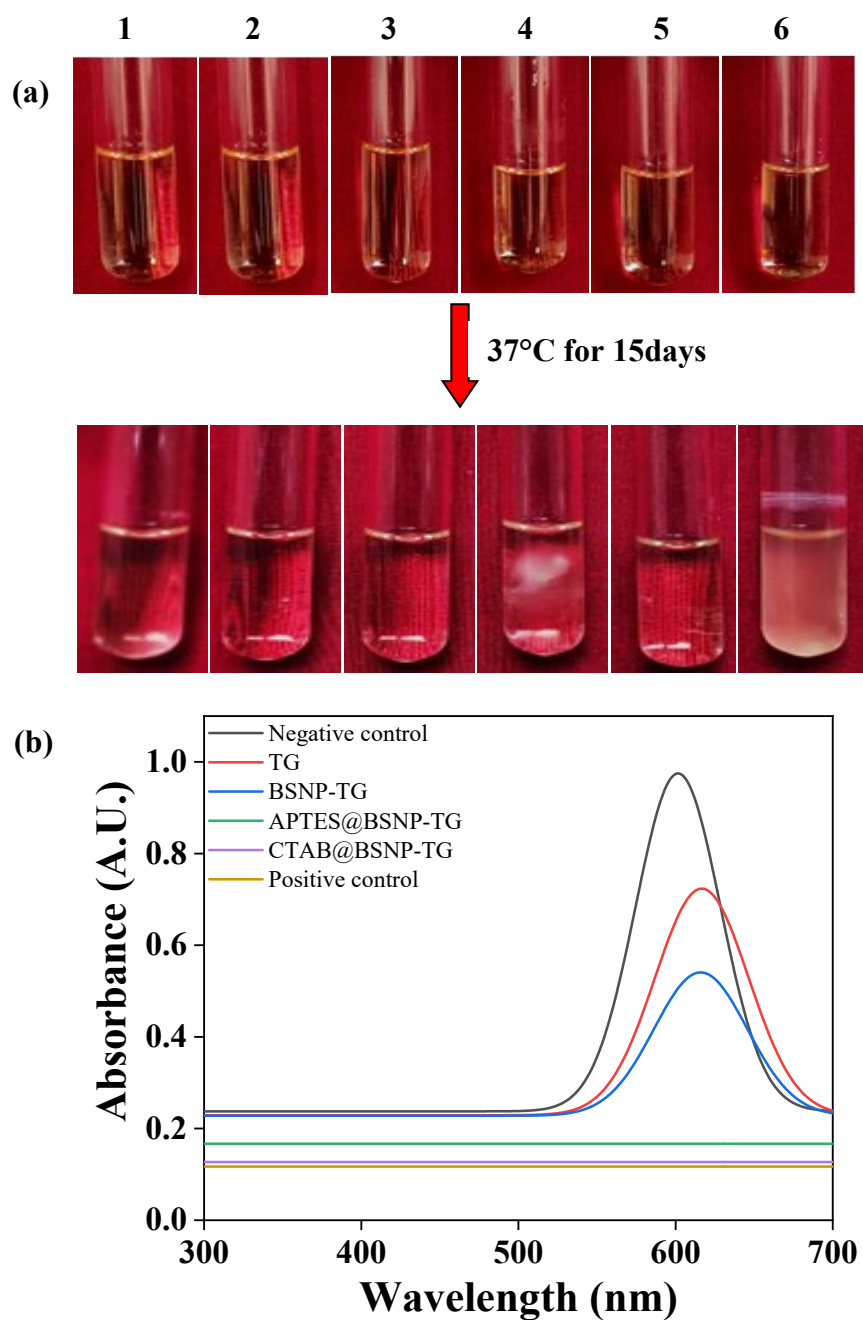
Antibacterial activity of synthetic silica NPs against *S. aureus* and (d) *P. aeruginosa*

Figure S6.



**Figure S6.** Variation in zeta potential of (a) *S. aureus* (from negative to positive) and (b) *P. aeruginosa* after interaction with NPs. DiSC<sub>35</sub>-based membrane depolarization assay kinetics of (c) *Pseudomonas aeruginosa* (d) *S. aureus* cells treated with 30 mg/mL of hydrogels.

**Figure S7.**



**Figure S7.** Secondary penetration assay of bacteria after treatment with different hydrogels in presence of (1) BSNP-TG, (2) APTES@BSNP-TG, (3) CTAB@BSNP-TG, (4) TG, (5) cotton plug (positive control), and (6) open test tube (negative control) at t=0 (top) and t = 15 days (bottom). (b) Quantification of turbid test tube media

**Figure S8**

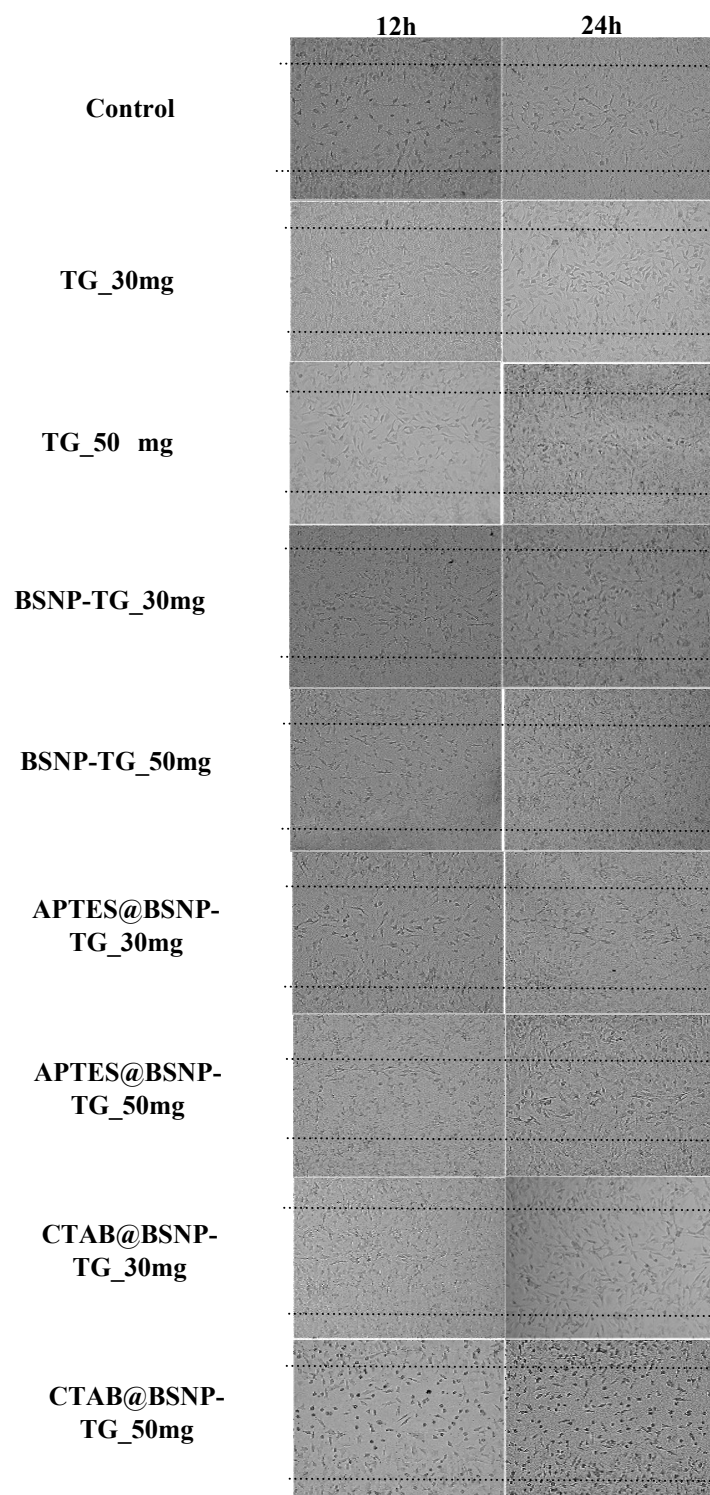


**Figure S8.** Cell migration assay of NIH-3T3 fibroblast at different time intervals *viz.*, 0, 12 and 24h after treating with PBS (control), TG, BSNP-TG, APTES@BSNP-TG, and CTAB@BSNP-TG with two different concentrations (30mg and 50mg).

## References

1. Burel, C.; Direur, G.; Rivas, C.; Purevdorj-Gage, L. Colorimetric detection of residual quaternary ammonium compounds on dry surfaces and prediction of antimicrobial activity using bromophenol blue. *Lett. Appl. Microbiol.*, 2021, 72, 358-365.
2. Sharma, C.; Shukla, A. K.; Acharya, A. Rational design of a FRET-based nanoprobe of gold-conjugated carbon dots for simultaneous monitoring and disruption of *Pseudomonas aeruginosa* biofilm through selective detection of virulence factor pyocyanin. *Environ. Sci. Nano*, 2021, 8, 1713-28.
3. Guliani, A.; Pooja; Verma, M.; Kumari, A.; Acharya, A. Retaining the 'essence' of essential oil: Nanoemulsions of citral and carvone reduced oil loss and enhanced antibacterial efficacy via bacterial membrane perturbation. *J. Drug Deliv. Sci. Technol.*, 2021, 61, 102243.
4. Kaur, R.; Thakur, N.S.; Chandna, S.; Bhaumik, J. Sustainable Lignin-Based Coatings Doped with Titanium Dioxide Nanocomposites Exhibit Synergistic Microbicidal and UV-Blocking Performance toward Personal Protective Equipment. *ACS Sustain. Chem. Eng.*, 2021, 9, 11223-11237.
5. Dadwal, V.; Bhatt, S.; Joshi, R.; Gupta, M. Development and characterization of controlled released polyphenol rich micro-encapsulate of *Murraya koenigii* bark extract. *Food Process Preserv.*, 2020, 44, e14438
6. Arno, M.C.; Inam, M.; Weems, A.C.; Li, Z.; Binch, A.L.; Platt, C.I.; ... O'Reilly, R.K. Exploiting the role of nanoparticle shape in enhancing hydrogel adhesive and mechanical properties. *Nat. Commun.*, 2020, 11, 1-9.

7. Singh, B.; Singh, J. Application of tragacanth gum and alginate in hydrogel wound dressing's formation using gamma radiation. *Carbohydr. Polym. Technol. Appl.*, 2021, 2, 100058-100068.
8. Liu, K.; Zhang, F.; Wei, Y.; Hu, Q.; Luo, Q.; Chen, C.; Wang, J.; Yang, Li.; Rifang, Luo Wang, Y. Dressing Blood-Contacting Materials by a Stable Hydrogel Coating with Embedded Antimicrobial Peptides for Robust Antibacterial and Antithrombus Properties. *ACS Appl. Mater. Interfaces*, 2021, 13, 38947-38958.
9. Walsh, B.J.; Thornton, S.C.; Penny, R.; Breit, S.N. Microplate reader-based quantitation of collagens. *Anal. Biochem.*, 1992, 203, 187-190.
10. Xu, Q.; Norman, J.T.; Shrivastav, S.; Lucio-Cazana, J.; Kopp, J.B. In vitro models of TGF- $\beta$ -induced fibrosis suitable for high-throughput screening of antifibrotic agents. *Am. J. Physiol.- Ren. Physiol.*, 293(2), F631-F640
11. Rovani, S., Santos, J. J., Corio, P., Fungaro, D. A. (2018). Highly pure silica nanoparticles with high adsorption capacity obtained from sugarcane waste ash. *ACS Omega*, 2017, 3, 2618-2627.
12. Franco, A.; De, S.; Balu, A.M.; Romero, A.A.; & Luque, R. Integrated Mechanochemical/Microwave-Assisted Approach for the Synthesis of Biogenic Silica-Based Catalysts from Rice Husk Waste. *ACS Sustain. Chem. Eng.*, 2018, 6, 11555-11562
13. Piela, A.; Żymańczyk-Duda, E.; Brzezińska-Rodak, M.; Duda, M.; Grzesiak, J.; Saeid, A.; ... Klimek-Ochab, M. Biogenic synthesis of silica nanoparticles from corn cobs husks. Dependence of the productivity on the method of raw material processing. *Bioorg. Chem.*, 2020, 99, 103773.

14. Buazar, F. Impact of biocompatible nanosilica on green stabilization of subgrade soil. *Sci. Rep.*, 2019, 9, 1-9.
15. Vaibhav, V.; Vijayalakshmi, U.; Roopan, S.M. Agricultural waste as a source for the production of silica nanoparticles. *Spectrochim. Acta-A: Mol. Biomol. Spectrosc.*, 2015, 139, 515-520
16. Gong, J.; Wang, L.; Wu, J.; Yuan, Y.; Mu, R.J.; Du, Y.; ... Pang, J. The rheological and physicochemical properties of a novel thermosensitive hydrogel based on konjac glucomannan/gum tragacanth. *LWT*, 2019, 100, 271-277.
17. Mallakpour, S.; Tabesh, F. Tragacanth gum based hydrogel nanocomposites for the adsorption of methylene blue: Comparison of linear and non-linear forms of different adsorption isotherm and kinetics models. *Int. J. Biol. Macromol.*, 2019, 133, 754-766.
18. Azarniya, A.; Tamjid, E.; Eslahi, N.; & Simchi, A. Modification of bacterial cellulose/keratin nanofibrous mats by a tragacanth gum-conjugated hydrogel for wound healing. *Int. J. Biol. Macromol.* 2019, 134, 280-289.
19. Singh, B.; Varshney, L.; Francis, S. Designing tragacanth gum based sterile hydrogel by radiation method for use in drug delivery and wound dressing applications. *Int. J. Biol. Macromol.*, 2016, 88, 586-602.
20. Kannan, R., Prabakaran, P., Basu, R., Pindi, C., Senapati, S., Muthuvijayan, V., & Prasad, E. Mechanistic study on the antibacterial activity of self-assembled poly (aryl ether)-based amphiphilic dendrimers. *ACS Appl. Bio Mater.*, 2019, 2(8), 3212-3224.

21. Upadhyay, A.; Kandi, R., & Rao, C. P. Injectable, self-healing, and stress sustainable hydrogel of BSA as a functional biocompatible material for controlled drug delivery in cancer cells. *ACS Sustain. Chem. Eng.* 2018, 6(3), 3321-3330.